



Population synthesis models and the VO

M. Salaris¹, S. Percival¹, S. Cassisi², and A. Pietrinferni²

¹ Astrophysics Research Institute Liverpool John Moores University 12 Quays House Birkenhead CH41 1LD, UK, e-mail: [ms;smp]@astro.livjm.ac.uk

² INAF-Osservatorio Astronomico di Collurania, Via M. Maggini, I-64100 Teramo

Abstract. Stellar population synthesis models (PSMs) are nowadays a fundamental tool to investigate the mechanisms of galaxy formation and evolution. We briefly review the fundamentals of PSM building and testing, list the main spectral and isochrone libraries currently available, and describe as a practical example the computation and testing of BaSTI PSMs. Important issues related to the implementation of population synthesis models into the Virtual Observatory are also sketched.

Key words. Astronomical data bases: miscellaneous - Stars: atmospheres - Stars: general - Galaxies: evolution - Galaxies: star clusters - Galaxies: stellar content

1. Introduction

Stellar population synthesis models (PSMs) are fundamental tools for interpreting the integrated light that we observe from unresolved stellar populations (nearby and high redshift galaxies, star clusters). A PSM provides the integrated spectrum of a stellar population, integrated magnitudes/colours plus mass-to-light ratios in various photometric bands and their evolution with time, for a specific star formation history (SFH) and stellar initial mass function (IMF).

In this contribution we discuss how a PSM is calculated (describing as an example the BaSTI population synthesis database) the necessary ingredients and related uncertainties, the question of how (if) it is possible to test PSMs on local resolved stellar populations, and some issues related to the inclusion of theoretical PSMs into the Virtual Observatory (VO).

Send offprint requests to: M. Salaris

2. Computation of a PSM

PSMs play a crucial role in investigations about formation and evolution of galaxies, by means of what we will define here as the 'inverse' and 'direct' approach, visualized in Figs. 1 and 2. In the inverse approach, photometric and spectroscopic observations of unresolved stellar populations produce empirical integrated spectra and/or colours/magnitudes that are compared to results from PSMs, to constrain the population SFH. This can be done for example by using integrated colour-colour diagrams that break the age-metallicity degeneracy (e.g., James et al. 2006), spectrophotometric indices, like the Lick system (e.g., Worthey et al. 1994), by fitting integrated spectra at intermediate resolution (e.g., Panter et al. 2003; Koleva et al. 2008), or broadband integrated magnitudes covering as much a large wavelength range as possible (e.g., Anders et al. 2004).

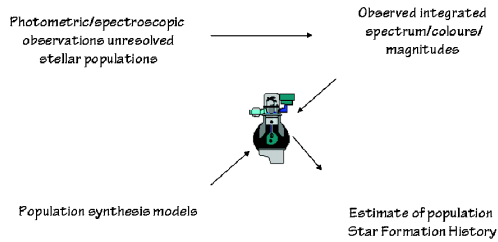


Fig. 1. Description of the inverse approach to constrain galaxy formation and evolution scenarios.

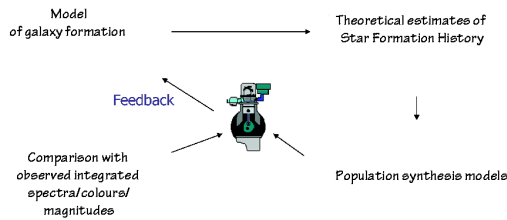


Fig. 2. Description of the direct approach to constrain galaxy formation and evolution scenarios.

The direct approach starts from a theoretical model for galaxy formation that predicts a specific SFH of the parent stellar population. PSMs convert this theoretical SFH into expected integrated photometric and spectroscopic properties, that are then compared to the observational counterpart. Eventual mismatches are used as guidelines to refine the theoretical galaxy formation model and the cycle is repeated. A (non-exhaustive) list of publicly available PSM archives is presented in Table 1.

One of the two main theoretical building blocks of a PSM is a library of stellar isochrones, that describe the predicted behaviour in the $L - T_{\text{eff}}$ plane of simple stellar populations (SSPs - single age, single metallicity stellar populations) covering a range of chemical composition and ages (t). Each point along an isochrone is specified by the local value of L , T_{eff} , the initial chemical composition (parameterized by $[\text{Fe}/\text{H}]$ for scaled-solar isochrones) and the mass M of the star evolving at that point. From L , T_{eff} and M one derives the stellar surface gravity g all along the isochrone, a quantity needed in order to pro-

Table 1. Main population synthesis model archives

BC03 (Bruzual & Charlot 2003)
Pegase (Le Borgne et al. 2004)
GALEV (Schulz et al. 2002)
Starburst99 (Leitherer et al. 1999)
SED@ (Delgado et al. 2005)
BaSTI (Percival et al. 2008)
Galadriel (Tantalo & Chiosi 2004)
Vazdekis (Vazdekis 1999)
Maraston (Maraston 2005)
Buzzoni (Buzzoni 2002)
Schiavon (Schiavon 2007)

duce the final integrated spectrum. The second main ingredient is a library of stellar spectra to transform L and T_{eff} into magnitudes, colours, spectra. Individual stellar spectra are defined in terms of T_{eff} , g and $[\text{Fe}/\text{H}]$. Together with these two main building blocks, an initial mass function (IMF) has to be specified. The IMF provides the number of stars at each point along the isochrone, given a value of the total stellar mass of the population. For each point along the isochrone, interpolations among the spectral library produces a stellar spectrum to be assigned to the evolving star, that is then rescaled according to the local number of objects predicted by the IMF. This procedure is repeated for each isochrone point, and the spectra added up to produce an integrated spectrum. At this point, if/when appropriate, one can apply corrections due to dust extinction, nebular emission, K-correction (see Fig.3). From this final spectrum line indices, integrated magnitude/colours, mass-to-light ratios can be then extracted.

3. Choices

As it should be obvious from the previous section, a number of choices have to be made before producing PSMs. The three main choices are the following:

- i) IMF: Functional form, universal or dependent on the properties (e.g., age, metallicity) of the stellar population ?

ii) Model/isochrone library: [Fe/H]-t-metal mixture-evolutionary phase coverage, mass loss history for massive stars, red giant branch (RGB) and asymptotic giant branch (AGB) stars

iii) Spectral library: empirical or theoretical. For both choices, crucial characteristics are resolution, λ - g -[Fe/H]-metal mixture- T_{eff} coverage. In case of theoretical libraries line lists and atmosphere modelling are two main issues. In case of empirical libraries S/N, flux calibration, determination of g - T_{eff} -[Fe/H] for the library stars are the the main uncertainties.

Table 2 summarizes several publicly available libraries of empirical and theoretical stellar spectra, and stellar evolution models/isochrones suitable for computing PSMs.

In the BaSTI (a Bag of Stellar Tracks and Isochrones) archive of stellar models and isochrones (Cordier et al. 2007) we have very recently included predictions for integrated spectra at low and intermediate resolution for SSPs, as described in detail by Percival et al. (2008). Our choices provide a working example of the issues confronting PSM builders.

We employed the isochrones described in Cordier et al. (2007), covering two metal mixtures (one scaled solar and one α -enhanced with $[\alpha/\text{Fe}] \sim 0.4$), 11 values of the metal mass fraction Z , from 0.0001 to 0.04 (the helium mass fraction Y increasing with Z as $\Delta Y/\Delta Z \sim 1.4$, starting from $Y=0.245$ at $Z=0.0001$), ages between ~ 30 Myr and 15 Gyr (or more), two alternative choices for the mass loss efficiency along the RGB and two choices for the treatment of convective cores during the Main Sequence. All isochrones reach either the end of the thermal pulsing phases along the AGB or carbon ignition, when appropriate.

To calculate low-resolution integrated spectra plus broadband integrated magnitudes, we made use of the ATLAS9 theoretical spectra, supplemented below 3500 K by the semiempirical BASEL library (see Table 2). For the thermal pulsing phase we employed the empirical spectra by Lancon & Mouhcine (2002). There is at present no single theoretical (or empirical) spectral library that can cover all the relevant parameter space. Tests described in Cordier et al. (2007) and Percival et al.

(2008) show that integrated magnitude/colours calculated combining these three sets of spectra produce satisfactory results, in spite of the inhomogeneity of the three libraries.

The situation is worse at higher resolutions (of the order of 1\AA or higher). Figure 4 displays the parameter space coverage (boxes) of the Munari theoretical spectral library that we have employed to produce our integrated spectra at 1\AA resolution. The coolest and brightest stars are not covered by this library, that stops at $T_{\text{eff}}=3500$ and $\log(g)=0.0$. On the same diagram, points represent stars used to build the Miles empirical spectral library, that has also a resolution of similar order of magnitude. The coverage is very sparse in some regions of the parameter space and again sections of the isochrones are not covered at all.

One would be tempted to implement at low temperatures the MARCS spectral library that has an adequate wavelength resolution and reaches lower values of T_{eff} (although it is limited to only 8000 K at high temperatures). Figure 5 displays a comparison between some of the Lick spectral indices computed with the Munari and an older version of the MARCS spectra (at this point in time new computations of low-temperature spectra are being included in the MARCS database). At common temperatures between 4000 and 5000 K and low gravities, differences between the predicted indices are very large, demonstrating the significant differences between the two sets of spectra. In this respect we wish to mention the paper by Martins & Coelho (2007), that presents a much more extensive comparison of this type, considering many of the spectral libraries listed in Table 2, both theoretical and empirical.

In Percival et al. (2008) we employed the sole Munari spectral library when producing integrated spectra at 1\AA resolution. Neglecting stars below $T_{\text{eff}}=3500$ makes these spectra of very limited use for λ above 6000\AA .

Two sample spectra at low- and at 1\AA resolution from the BaSTI website are shown in Fig. 6. In our calculations we have employed the Kroupa (2001) universal IMF.

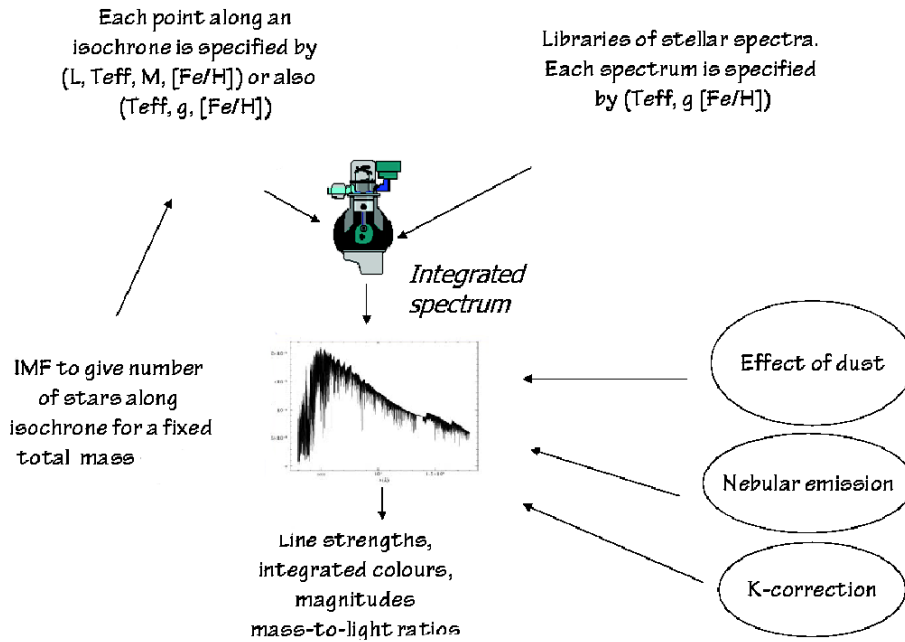


Fig. 3. Schematic description of how to compute a PSM

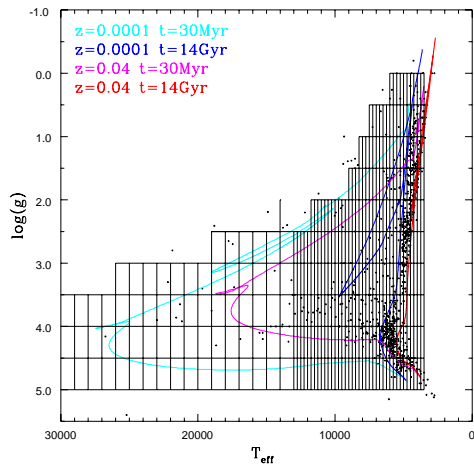


Fig. 4. $T_{\text{eff}}-g$ coverage of the Munari theoretical spectral library and the Miles empirical one, compared to two pairs of theoretical isochrones with extreme values of age and metallicity.

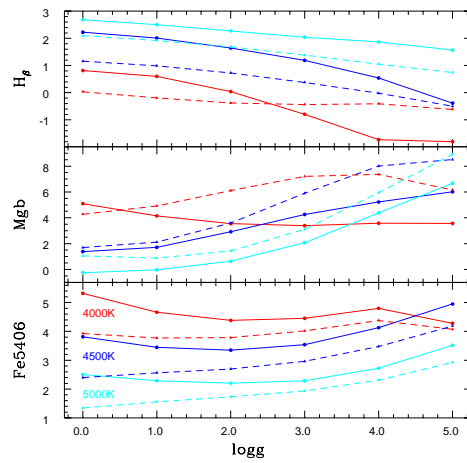
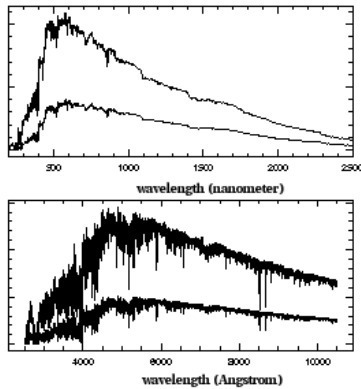


Fig. 5. Comparison of selected Lick indices computed from the Munari (dashed lines) and MARCS (solid lines) spectral libraries at a subset of common temperatures.

Table 2. Main spectral and isochrone libraries for population synthesis modelling

Empirical spectra	Theoretical spectra	Isochrones
STELIB (Le Borgne et al. 2004)	Munari (Munari et al. 2005)	BaSTI (Cordier et al. 2007)
ELODIE (Prugniel & Soubiran 2001)	Coelho-IAG (Coelho et al. 2005)	Padua (Bertelli et al. 2008)
INDO-US (Valdes et al. 2004)	Martins (Martins et al. 2005)	DSEP (Dotter et al. 2008)
MILES (Sánchez-Blázquez et al. 2006)	MARCS (Gustafsson et al. 2008)	Y2 (Yi et al. 2003)
UVES-POP (Jehin et al. 2005)	PHOENIX (Brott & Hauschildt 2005)	Geneva (Lejeune & Schaerer 2001)
NGSL (Gregg et al. 2004)	ATLAS9 (Castelli & Kurucz 2004)	Victoria (Bergbusch & Vandenberg 2001)
Pickles (Pickles 1998)		
BaSEL (semiemp.) (Westera et al. 2002)		

**Fig. 6.** Sample low- (upper panel) and intermediate-resolution (lower panel) integrated spectra for stellar populations with $[Fe/H]=0.06$, $t=3$ and 10 Gyr, respectively.

4. Tests

Once a PSM is calculated, it is very important to test whether its application to integrated spectra and/or magnitudes of local resolved objects – most notably star clusters in the Galaxy – provide results in agreement with the colour-magnitude-diagram (CMD) analy-

sis with isochrones (ideally using the same set of isochrones and bolometric corrections coming from the same spectral library used to compute the PSM) and metal abundances from stellar spectroscopy. Unfortunately this type of tests is hampered by at least three main factors:

i) Uncertainties of spectroscopic metallicities:

There are large discrepancies between cluster metallicity scales (see, e.g., the discussion in Percival et al. 2008). Well studied objects like the Galactic globular clusters M3 and M5 show differences of ~ 0.3 dex between different $[Fe/H]$ estimates. A metal poor cluster like M68 displays a ~ 0.4 dex range of $[Fe/H]$ values. Taking a mean value of the determinations for each cluster is not meaningful, given that differences among authors are mainly systematic. Also, $[\alpha/Fe]$ spectroscopic estimates do not exist for many clusters. A related important issue is the presence of the well known CN and ONa anticorrelations in the metal mixture of stars within a single cluster (see, e.g., the review by Gratton et al. 2004, and references therein). There is now general agreement that these abundance patterns are of primordial origin. The integrated spectrum of a cluster is therefore composed of individual spectra

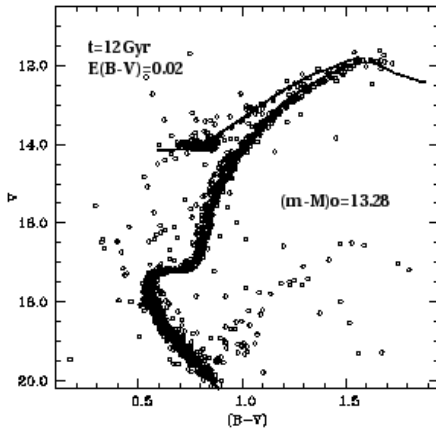


Fig. 7. Fit to 47 Tuc CMD (Stetson 2000) with $[\text{Fe}/\text{H}] = -0.7$, α -enhanced BaSTI isochrones and Zero Age HB.

with a range of values for the very important CNONa elements, with the Fe abundance being constant for all stars. As a consequence, it is very difficult to interpret the strength of all line indices involving these 4 elements, because in a cluster the exact proportions of stars with a certain set of CNONa abundances, and their location in the CMD, are known only for small samples of objects.

ii) Horizontal Branch morphology:

The presence of blue Horizontal Branch (HB) stars affects integrated magnitudes/colours and Balmer lines, and can produce spuriously young ages for clusters with an extended blue HB if this is not included in the theoretical modelling. A detailed synthetic modelling of the HB colour extension for each of the observed clusters is therefore in principle necessary, but it is difficult to implement in practice and would be computationally very time consuming to model all the different possibilities. This approach also assumes that one knows in advance the appropriate morphology required and this of course is not possible for unresolved stellar clusters.

iii) Statistical fluctuations of integrated magnitudes/colours and spectral indices:

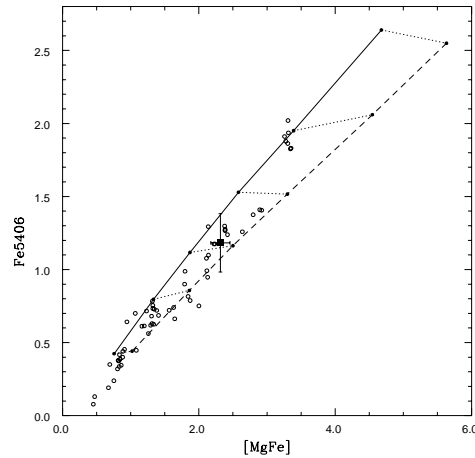


Fig. 8. Theoretical $[\text{MgFe}]$ -Fe5406 diagram compared to data for a sample of Galactic globular clusters (observed spectra from Schiavon et al. 2005). The solid line corresponds to 14 Gyr scaled solar BaSTI models, the dashed line to α -enhanced ones. The point corresponding to 47 Tuc is displayed with attached observational error bars.

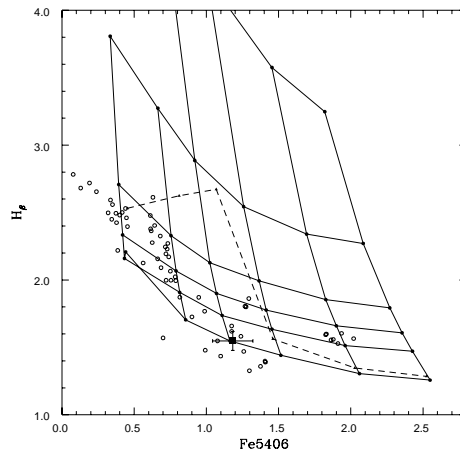


Fig. 9. Fe5406- H_β diagram from α -enhanced BaSTI models. Ages (in Gyr) and $[\text{Fe}/\text{H}]$ are labeled. The dashed line corresponds to the predicted indices for a 14 Gyr population with a higher mass loss efficiency along the RGB (i.e. a bluer HB at low metallicities). Points corresponds to the same clusters displayed in Fig. 8. 47 Tuc is displayed with attached observational error bars.

The analytical computation of integrated spectra described above is the standard procedure followed in the literature. This is however strictly valid in the limit of an infinite number of stars. The analytical computation implies that all points along the isochrones are smoothly populated by a number of stars that can be equal to just a fraction of unity in case of fast evolutionary phases, whereas in real clusters the number of objects at a point along the CMD is either zero or a multiple of unity. When the number of stars in the observed population is not large enough to sample smoothly all evolutionary phases, statistical fluctuations of star counts will arise. This means that an ensemble of SSPs with the same total mass, t and Z will show a range of integrated spectra (hence magnitudes and colours) due to stochastic variations of the number of objects populating the faster evolutionary phases. In case of intermediate/old SSPs they are the upper RGB and AGB. The magnitude of these fluctuations will be larger in the wavelength ranges most affected by the flux emitted by RGB and AGB stars, typically the near-IR and longer wavelengths, but also line indices centered at shorter wavelengths can be affected, as we will see below.

Figure 7 displays the isochrone and zero age horizontal branch fit to the Galactic globular cluster 47 Tuc, using the BaSTI isochrones described in Cordier et al. (2007). Considering estimates from various authors, this cluster has a reasonably well established $[\text{Fe}/\text{H}] = -0.7 \pm 0.1$. As a test of the BaSTI PSM we show in Fig. 8 the $\text{Fe}5406$ – $[\text{Mg}/\text{Fe}]$ plane, that is a diagnostic of $[\text{Fe}/\text{H}]$ and the degree of α -enhancement, fairly independent of the cluster age (e.g., Percival et al. 2008, and references therein). Points corresponding to 47 Tuc (with error bars) and additional Galactic globular clusters are overimposed. Figure 9 shows the same GC data points on the α -enhanced $\text{Fe}5406$ – H_β $[\text{Fe}/\text{H}]$ and age diagnostic. The intermediate metallicity clusters generally span the ~ 10 – 14 Gyr age range (within the errors), whereas the more metal poor clusters all seem to scatter to lower ages. This is most likely to be due to the blue extension of their HB. To illustrate the potential effect of having blue

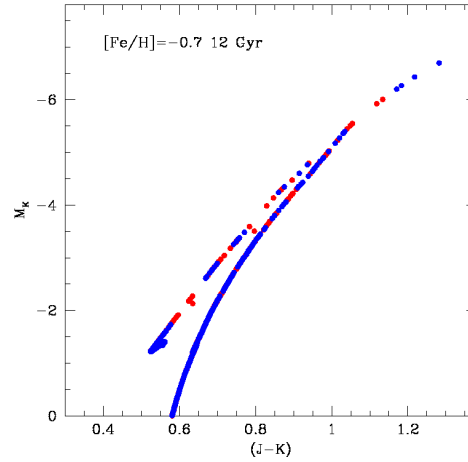


Fig. 10. Two Monte Carlo realizations (red and blue points) of the CMD for a globular cluster with a typical mass of $1.5 \cdot 10^5 M_\odot$ and the labeled $[\text{Fe}/\text{H}]$ and age.

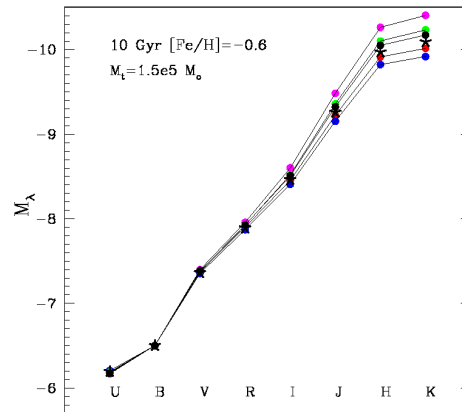


Fig. 11. Integrated magnitudes from 4 Monte Carlo realizations of a globular cluster with the labeled parameters. Black symbols display the values for an analytical integration along the isochrone

HBs due to increased mass loss on the RGB, we have overplotted the 14 Gyr line calculated using a higher mass loss efficiency along the RGB. This clearly demonstrates the large increase in the strength of the H_β line which can

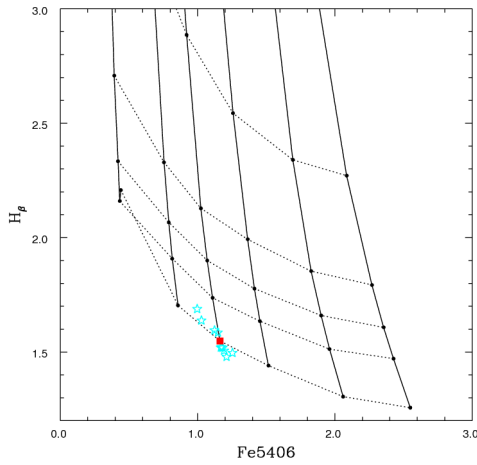


Fig. 12. Integrated Fe5406- H_β indices for several Monte Carlo realizations of a globular cluster with total mass equal to $1.5 \cdot 10^5 M_\odot$, $[\text{Fe}/\text{H}] = -1.01$, α -enhanced, $t = 14$ Gyr. The red square displays the value expected from an analytical integration.

lead to spuriously young ages. Within the error bars, for the case of 47 Tuc Figs. 8 and 9 provide age, $[\text{Fe}/\text{H}]$ and α -enhancement fairly consistent with spectroscopy and CMD fitting.

47 Tuc is a moderately massive globular cluster, with a total mass a factor of ~ 10 larger than the typical mass of Galactic globulars, equal to $\sim 1.5 \cdot 10^5 M_\odot$. The effect of statistical fluctuations is smaller for this cluster, but still non negligible especially in integrated near-IR magnitudes, and associated colours (see, e.g., Salaris & Cassisi 2007). Figures 10, 11 and 12 display the effect of statistical fluctuations in star counts on the CMD, integrated magnitudes and line indices for synthetic globulars with a total mass of $1.5 \cdot 10^5 M_\odot$. One can see how statistical fluctuations alter the stellar distribution along the brightest and coolest evolutionary phases, that translates into a very large spread in the predicted integrated near-IR magnitudes, of the order of ≈ 1 mag in K . This source of statistical spread makes very difficult to employ integrated near-IR magnitudes and colours (necessary to break the age-metallicity degeneracy) to determine age and metallicity of individual unresolved globular clusters with

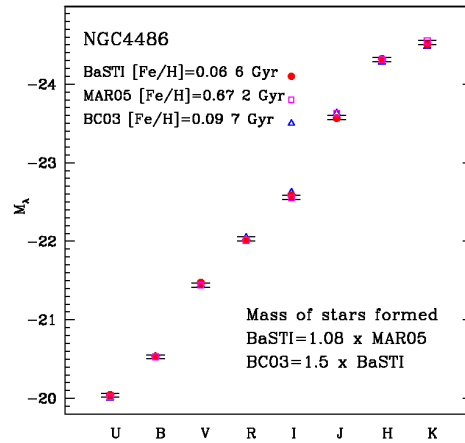


Fig. 13. Best fit of the integrated magnitudes from U to K for an unresolved elliptical galaxy (data from Michard 2005), using SSPs from three different PSMs.

masses of this order. Even clusters a factor of 10 more massive are subject to non negligible fluctuations in their near-IR magnitudes.

Fluctuations of this origin are not restricted to colours. In fact they affect also line indices used as age and metallicity diagnostics, as displayed in Fig. 12. Intrinsic uncertainties of the order of 0.3 dex in $[\text{Fe}/\text{H}]$ seem unavoidable for globular clusters with this total mass, as well as indeterminations also on the age estimate. This indetermination in the predicted line indices (that of course depend on the total cluster mass) should be added to the observational uncertainties when estimating age and metallicities from these line index diagnostics.

5. PSM and the VO

As shown in Table 1, there is a large selection of PSMs available to researchers. These PSMs all use different combinations of the inputs summarized in Table 2 and often produce quite different results when applied to the study of extragalactic stellar populations. Figure 13 shows just an example of applying BaSTI, BC03 and Maraston integrated magnitudes to fit the integrated magnitudes from U

to K of the elliptical galaxy NGC4486 (data by Michard 2005).

Implementation in the VO of a large range of PSMs would be ideal to test them (with all the limitations sketched above) against resolved objects in an homogeneous fashion, to facilitate their use to investigate unresolved extragalactic populations and gauge quantitatively the uncertainties related to theory. An implementation with this purpose in mind will have to address a number of issues:

- i) Standardization of the outputs and data description.
- ii) Efficient interface with tools for analysis of retrieved data.
- iii) Identification of models/search of parameter space during the analysis.
- iv) Ownership, updates

Efforts in this direction are being made by the BaSTI collaboration regarding at the moment only the stellar model database, and the TSAP (Theoretical Spectra Access Protocol) service developed at LAEFF-Madrid.

A further step could be to use VO capabilities to implement several available model and spectral libraries with flexibility to choose among several possible combinations for computing from scratch a specific PSM to best tackle the problem at hand. This development would have to face a similar set of issues:

- i) Standardization of formats and data description of population synthesis building blocks.
- ii) Keep track of the characteristics of each library. Search within the whole parameter space for the combination(s) most suited to interpret the data: resolution, λ (or broadband filter) coverage, etc.
- iii) Option to test the final PSM on template objects.
- iv) Ownership, updates.

6. Conclusions

Stellar population synthesis models are a fundamental tool to investigate the mechanisms of galaxy formation and evolution. We have briefly reviewed the fundamentals of PSM building and testing, listed the main spectral and isochrone libraries, and described as a

practical example the computation and testing of BaSTI PSMs. Important issues related to the implementation of PSMs into the VO have been also sketched.

The inclusion of PSMs within the VO will need a concerted effort from both 'producers' and 'users' of PSMs, in order to solve the problems mentioned in the previous section. If these issues are addressed and solved, the VO could provide an extremely powerful instrument not only to exploit and test existing PSMs, but also to guide future developments of stellar population synthesis.

Acknowledgements. M.S. would like to thank the organizers for their invitation and the UK-VO for financial support.

References

- Anders, P., Bissantz, N., Fritze-v. Alvensleben, U. & de Grijs, R. 2004, MNRAS, 347, 196
- Brott, I. & Hauschildt, P. H. 2005, in Turon C., O'Flaherty K. S., Perryman M. A. C., eds, The Three-Dimensional Universe with Gaia: A PHOENIX Model Atmosphere Grid for Gaia, ESA SP-576. ESA, Noordwijk, p. 565
- Bergbusch, P. A. & Vandenberg, D. A. 2001, ApJ, 556, 322
- Bertelli, G., Girardi, L., Marigo, P. & Nasi, E. 2008, A&A, 484, 815
- Bruzual, G. & Charlot, S. 2003, MNRAS, 344, 1000
- Buzzoni, A. 2002, AJ, 123, 1188
- Castelli, F. & Kurucz, R. L. 2004, in Proceedings of the IAU Symp. No 210; IAU Symp. No 210, Modelling of Stellar Atmospheres, eds. N. Piskunov et al. 2003, poster A20 (arXiv:astro-ph/0405087)
- Coelho, P., Barbuy, B., Melendez, J., Schiavon, R. P. & Castilho, B. V. 2005, A&A, 443, 735
- Cordier, D., Pietrinferni, A., Cassisi, S. & Salaris, M. 2007, AJ, 133, 468
- Delgado, R. M. G., Cerviño, M., Martins, L. P., Leitherer, C. & Hauschildt, P. H. 2005, MNRAS, 357, 945
- Dotter, A., Chaboyer, B., Jevremovic, D., Kostov, V., Baron, E. & Ferguson, J. W. 2008, 178, 89

- Gratton, R., Sneden, C. & Carretta, E. 2004, *ARA&A*, 42, 385
- Gregg, M. D., et al. 2004, *Bull. Am. Astron. Soc.*, 36, 1496
- Gustafsson, B., Edvardsson, B., Eriksson, K., Joergensen, U. G., Nordlund, A. & Plez, B. 2008, *A&A*, 486, 951
- Leitherer, C., Schaerer, D., Goldader, J. D., Gonzalez Delgado, R. M., Robert, C., Kune, D. F., de Mello, D. F., Devost, D., & Heckman, T. M. 1999, *ApJS*, 123, 3
- James, P. A., Salaris, M., Davies, J. I., Phillipps, S. & Cassisi, S. 2006, *MNRAS*, 367, 339
- Jehin, E., Bagnulo, S., Melo, C., Ledoux, C. & Cabanac, R. 2005, in Hill V., Franois P., Primas F., eds, *IAU Symp. 228, The UVES Paranal Observatory Project: A Public Library of High Resolution Stellar Spectra* Cambridge Univ. Press, Cambridge, p. 261
- Koleva, M., Prugniel, Ph., Ocvirk, P., Le Borgne, D. & Soubiran, C. 2008, *MNRAS*, 385, 1998
- Kroupa, P. 2001, *MNRAS*, 322, 231
- Lancon, A. & Mouhcine, M. 2002, *A&A*, 393, 167
- Le Borgne J.-F., et al., 2003, *A&A*, 402, 433
- Le Borgne, D., Rocca-Volmerange, B., Prugniel, P., Lancon, A., Fioc, M. & Soubiran, C. 2004, *A&A*, 425, 881
- Lejeune, T. & Schaerer, D. 2001, *A&A*, 366, 538
- Lejeune, T., Cuisinier, F. & Buser, R., 1998, *A&AS*, 130, 65
- Maraston, C. 2005, *MNRAS*, 362, 799
- Martins, L. P., Delgado, R. M. G., Leitherer, C., Cervinõ, M. & Hauschildt, P. 2005, *MNRAS*, 358, 49
- Martins, L. P. & Coelho, P. 2007, *MNRAS*, 381, 1329
- Michard, R. 2005, *A&A*, 429, 819
- Munari, U., Sordo, R., Castelli, F. & Zwitter, T. 2005, *A&A*, 442, 1127
- Panther B., Heavens A. F., & Jimenez R. 2003, *MNRAS*, 343, 1145
- Percival, S. M., Salaris, M., Cassisi, S. & Pietrinferni, A. 2008, *ApJ*, in press
- Pickles, A.J. 1998, *PASP*, 110, 863
- Prugniel, P. & Soubiran, C. 2001, *A&A*, 369, 1048
- Salaris, M. & Cassisi, S. 2007, *A&A*, 461, 493
- Sánchez-Blázquez, P., et al. 2006, *MNRAS*, 371, 703
- Sandquist, E. L. 2004, *MNRAS*, 347, 101
- Schiavon, R. P. 2007, *ApJS*, 171, 146
- Schiavon, R. P., Rose, J. A., Courteau, S. & MacArthur, L. A. 2005, *ApJS*, 160, 163
- Schulz J., Fritze-v. Alvensleben U., Möller C. S. & Fricke K. J. 2002, *A&A*, 392, 1
- Stetson, P. B. 2000, *PASP*, 112, 925
- Tantalo, R. & Chiosi, C. 2004, *MNRAS*, 353, 405
- Valdes, F., Gupta, R., Rose, J., Singh, H. & Bell, D., 2004, *ApJS*, 152, 251
- Vazdekis, A. 1999, *ApJ*, 513, 224
- Westera, P., Lejeune, T., Buser, R., Cuisinier, F. & Bruzual, G. 2002, *A&A*, 381, 524
- Worthey G., Faber S., González J. & Burstein D., 1994, *ApJS*, 94, 687
- Yi, S. K., Kim, Y.-C. & Demarque, P. 2003, *ApJS*, 144, 259